DFT Studies on Schiff Base Formation of Vitamin B$_6$ Analogues

Antoni Salvà, Josefa Donoso,* Juan Frau, and Francisco Muñoz*

Departament de Química, Universitat de les Illes Balears, Ctra. Valldemossa, km 7.5,
07122 Palma de Mallorca, Illes Balears, Spain

Received: March 26, 2003; In Final Form: July 2, 2003

A comprehensive study of Schiff base formation of vitamin B$_6$ analogues by using DFT calculations (B3LYP/6-31+G*) and a study of the topology of the density charge function of the optimized structures according to Bader's AIM theory are carried out. Vitamin B$_6$ analogues for the gas-phase calculations include one auxiliary water molecule. These calculations result in the description of the geometries of all the intermediates and transition structures along the reaction pathway, which can be divided in three parts: carbinolamine formation, dehydration, and imine formation. The carbinolamine is the main intermediate, and dehydration is the limiting step of the reaction, in accordance with experimental evidence. The details of the mechanism of carbinolamine formation highlights the key role of the auxiliary water molecule of the molecular complex as a true reactive for allowing the nucleophilic attack of the incoming amine to the carbonyl group.

I. Introduction

Pyridoxal phosphate is a key coenzyme in the metabolism of amino acids. Racemization, transamination, decarboxylation and β-elimination are reactions in which PLP-dependent enzymes are involved.[1−4] In such enzymes, a primary amine group of a lysine residue[5] attacks the aldehyde function of the pyridoxal phosphate to form an imine in a Schiff base formation reaction.

The generally accepted mechanism for this reaction was proposed by Snell and Braunstein[6,7] and consists of the addition of the amine to a carbonyl compound to give an intermediate carbinolamine that loses one molecule of water to produce the imine.[8]

Although carbinolamines have proved difficult to observe in studies of PLP Schiff base formation, experimental evidence[9−11] supported the occurrence of such intermediate and the location of the rate-limiting step of the whole reaction in its dehydration. It is also known[12−15] that carbinolamine formation is a multistep process that involves zwitterionic intermediates in which internal proton transfers play a significant role.

It has been suggested that in enzymatic reactions of transamination and decarboxylation, these intermediates seem to be often involved in acid−base tautomer equilibria of quinonoid structures of Schiff base compounds.[16] It was shown for several α-amino acid decarboxylases that a single deuterium atom was incorporated from deuterium oxide in product amines, and that these asymmetrically labeled products were enantiomerically pure.[17] Experimental work established the environmental conditions required for the occurrence of Schiff base formation reaction[18] as well as which are the most stable tautomers for PLP in different pH and solvation conditions.[19−27]

Quantum mechanics calculations onto a reactive system can provide a detailed description of the intermediates and transition state geometries involved in the reaction. Early theoretical studies on the electronic structures of Schiff bases suggest that there are considerable π electron charges on the carbon atoms that form part of the imine skeleton, rendering their properties similar to those of atoms with a lone pair of electrons in the plane of the molecule. For this reason, electrophillic reagents, particulary protons, can attack these atoms.[28] This idea is summarized as the "electron sink" concept. This paradigm explains why carbanionic intermediates are stabilized by the extended conjugated π-electron system of the pyridine ring of PLP.[16] As far as PLP is concerned, Nero et al.[29] studied the main PLP intermediates involved in the transamination mechanism using the AM1 semiempirical molecular orbital method. Alagona et al.[30] focused their interest on the ability of carbanion formation on substrates including PLP. Bach et al.[31] have performed ab initio calculations regarding the reactivity of decarboxylation in the PLP-dependent process. In their work, these authors conclude that the fundamental role of the pyridoxyl ring in the overall process studied (decarboxylation) is to provide a neutral but zwitterionic tautomer of the substrate as a consequence of general acid catalysis that diminishes the energy gap between the ground-state structure and the transition structure. Toney,[32] by using semiempirical methods, has estimated the relative contribution of protonation of the pyridine nitrogen to the stabilization of the transition state structures leading to isomers of PLP and its analogues interacting with a carboxylic acid at the pyridine nitrogen. In this study, we focus the catalytic power of pyridoxal phosphate of pyruvoyl-dependent carboxylases in the simple pyruvoyl group.

A PM3 study regarding Schiff base formation of a PLP analogue with methylamine in gas phase and using two solvation models has been reported.[33] At this level of theory, we concluded from this work that one water molecule has a key role in the reactive complex for the achievement of reliable reaction barriers in the nucleophilic attack of the incoming amine onto the carbon of the carbonyl group.

In this work, the reactivity of PLP as regards to Schiff base formation with amino acids will be discussed by means of the description of the energy, the geometry, and the topology of the charge density function of the intermediate and transition state structures involved in such reaction. This information provides a detailed energy profile for Schiff base formation that matches conclusions which have been obtained experimentally.

---

* Corresponding authors. E-mail: dqufmi0@uib.es.

SCHEME 1. Scheme of the Schiff Base Formation[a]
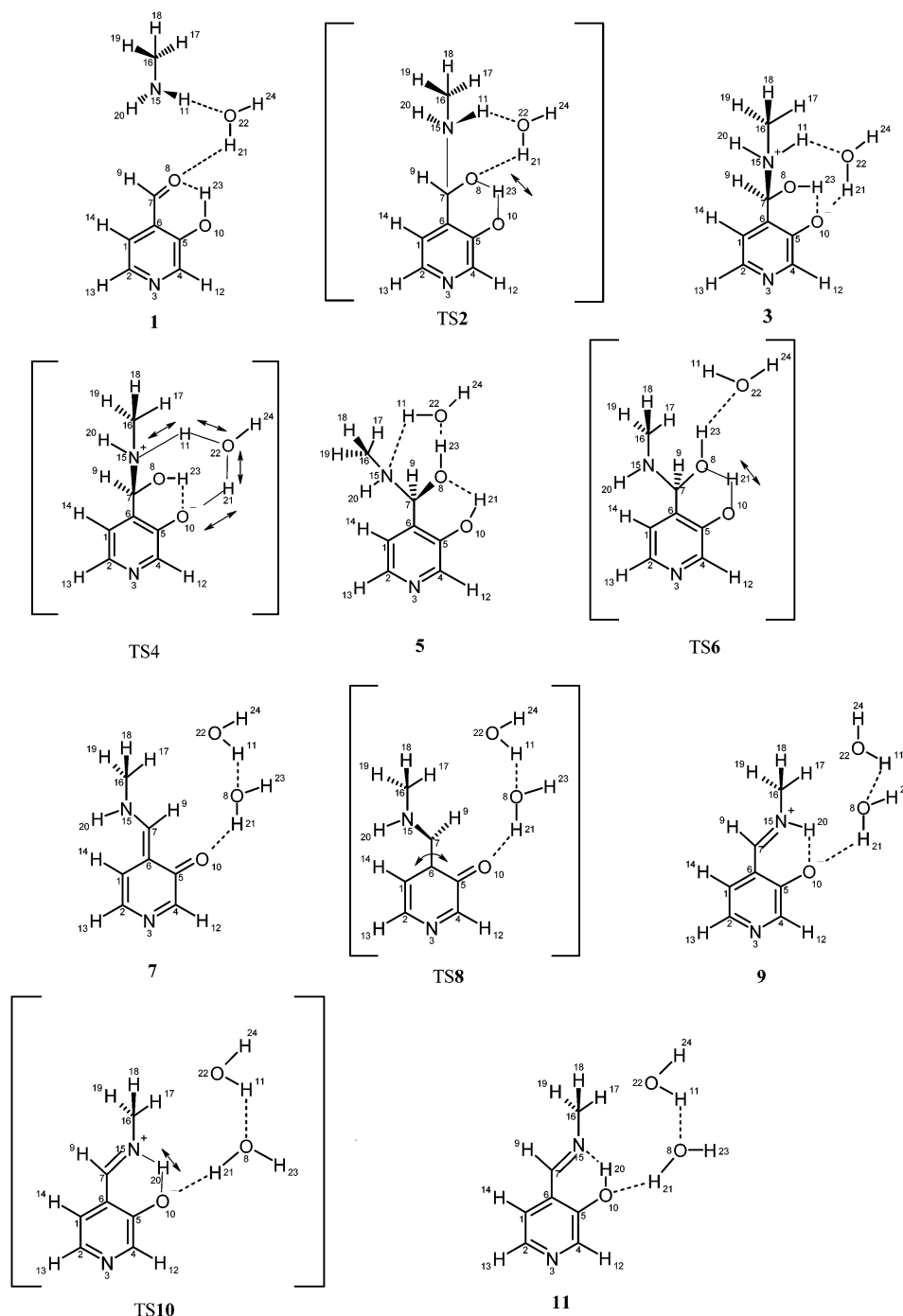
[a] Hydrogen bonds are represented as bold dotted lines while in transition state structures thin lines represent the bonds connecting nuclei which take part significantly in the transition state vector regarding the imaginary vibration. The main direction of this vibration is indicated by means of an arrow.

II. Methodology

A molecular complex consisting of 4-pyridinaldehyde, methylamine, and one water molecule was chosen as the model compound to study the Schiff base formation from PLP and one molecule with a free amino group. The purpose of including one water molecule in the model molecular complex was not the simulation of a water solvation environment but its consideration as a reactive species for the proceeding of the reaction. Previous theoretical studies on reactions involving a nucleophilic approach on carbonyl carbons established the need for the consideration of the solvent in order to avoid the lack of potential barrier when two molecules interact this way.[34−36]

DFT calculations were performed using the Gaussian94 program package[37] running in a Silicon Graphics Octane computer. All structures were fully optimized at the B3LYP level of theory.[38] Density functional theory methods with the exact exchange in hybrid form, in particular B3LYP, offer geometrical parameters, also for hydrogen bonds, in better accordance with MP2 data than results of HF calculations.[39,40] The 6-31+G* basis set has been used in this study. Polarized and diffuse basis functions for heavy atoms were included to ensure reliable results for small charge-localized charged atoms.

Reaction coordinates were used with full optimization of every parameter until the desired steady-state point was reached.
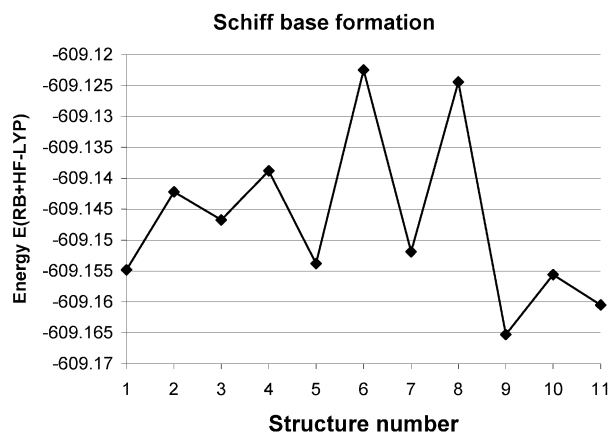
DFT Studies on Schiff Base Formation

J. Phys. Chem. A, Vol. 107, No. 44, 2003 **9411**

Figure 1. Energy profile for the reaction. Energy is in au.

TABLE 1: Energies (RB + HF-LYP) and Free Energies (Sum of Electronic and Thermal Free Energies) for Each of the Structures of the Reaction Path from the Standard Thermochemistry Output of a Frequency Calculation^a

structure	E(RB+HF-LYP)	$\epsilon_o + G_{corr}$
1	−609.154830	−609.006965
2	−609.142201	−608.986934
3	−609.146724	−608.986508
4	−609.138804	−608.983584
5	−609.153783	−608.994946
6	−609.122493	−608.970785
7	−609.151885	−609.000576
8	−609.124409	−608.972300
9	−609.165285	−609.014362
10	−609.155586	−609.009781
11	−609.160472	−609.011290

^{a} ϵ_0 is the total electronic energy and G_{corr} is the thermal correction to Gibbs free energy. All energies are in au.

Further vibrational analyses were performed on all optimized structures in order to characterize them as minima or saddle points in the energy hypersurface. All minima showed all the force constants positive, while saddle points had one, and only one, imaginary force constant. For the latter structures, IRC calculations were performed along the transition vector defined by the vibration mode of this imaginary frequency in order to assess that the saddle point structure connected downhill the corresponding forward and backward minima. This methodology allowed the identification of reaction intermediates and transition state structures along the reaction path.

Further, using the electron-correlated (B3LYP/6-31+G*) wave function of each intermediate and transition state structure, a topological study of the density charge function in order to locate bond, ring and cage critical points, was performed according to Bader's AIM theory[41] using the AIM2000 program[42] running in a PC. Molecular paths connecting bond critical points (BCP) and bond and ring critical points (RCP) were also computed for each of the structures along the reaction path found.

III. Results and Discussion

The structures found allow the outline of a detailed chemical path for the formation of a Schiff base between the pyridoxal phosphate model compound and a free amine. This process, shown in Scheme 1, can be described by means of three main steps, each one of them involving several intermediates and transition state structures: carbinolamine formation (structures **1**–**5**), dehydration (structures **5**–**7**) and imine formation (structures **7**–**11**). The energy profile appears in Figure 1. The energies and the free energies (sum of electronic and thermal free energies) are listed for each structure in Table 1.

A. Carbinolamine Formation. The starting point of this multistep process is structure **1**, in which the incoming amine has to attack nucleophilicaly the carbonyl carbon labeled as C7. The approximation of the amine is performed in such a way that the angle N15−C7−C6 is 104° (see the relevant geometrical data for all the structures in Table 2) at a distance N15−C7 of 2.911 Å. Even at this large distance, a bond critical point (BCP1 in Figure 2) was found in Bader's sense between both atoms, which indicates the existence of an interaction.

To assess univocally that the BCP found is related to the atoms that presumably participate in such interaction, a maximum electron density path connecting both nuclei, called bond path, is looked for. This bond path between N15 and C7 is outlined in Figure 2. The location of BCP1 proves this interaction prior to the nucleophilic attack of the incoming amine

to the carbonylic carbon. In this initial structure, an intramolecular hydrogen bond (1.801 Å) is established between H23 of the OH group on the pyridine ring and the carbonylic oxygen O8. Besides, the auxiliary water molecule is double-bridged to the incoming amine and the oxygen of the carbonyl group through the formation of two hydrogen bonds, H11−O22 (2.128 Å) and H21−O8 (1.901 Å). Each of these two interactions and their polar character are confirmed by the location of respective BCPs (BCP2 and BCP3 in Figure 2).

The analysis of the topology of the charge density function also allows the location of ring critical points (RCP), which have the lowest values of the charge density in the plane of a ring formed by the participating nuclei. For this initial structure **1**, in addition to the RCP that one can expect in the middle of the pyridine ring plane (RCP1 in Figure 2), the network of hydrogen bonding results also in the presence of two additional RCPs, as it can be seen in Figure 2: one corresponding to the carbonyl and hydroxyl group hydrogen-bonding network, which lays on the same plane as the pyridine ring (RCP2); a second one, which is related to the hydrogen-bonding network formed with the incoming amine, the water molecule, and the carbonyl and hydroxyl groups of PLP (RCP3). This latter RCP is located on a plane orthogonal to the pyridine ring. Ring−bond paths connecting BCPs and RCPs have also been found.

As can be seen from the free energy values of Table 1, this molecular complex is clearly more stable than the next intermediate (0.020457 au, 12.8 kcal/mol).

If a reaction coordinate calculation for the approaching path of N15 to C7 is performed from this initial structure 1, it shows no reaction barrier and the optimized structure reverses to the initial reactants. Instead, the nucleophilic attack of N15 to C7 takes place in an indirect way. From **1**, the system evolves to the transition state structure **2** with an energy barrier of 0.0126287 au (7.92 kcal/mol). In TS2, H23, the hydrogen of the OH group on the pyridine ring is transferred to the carbonyl oxygen O8. As a result of this transfer, a change of orientation of the double-bonded hydrogen bonding of the water molecule is observed.

A further insight in the arrangement of the bond and ring critical points and the paths connecting them in this structure reveals the apparition of a ring−bond path connecting RCP3 and BCP1. As a result of the achievement of TS2 through the hydrogen transference described above, the bond length between N15 and C7 nuclei lowers to 1.680 Å.

Downhill from this transition state structure, the system evolves to the adduct form **3**. The geometry of this structure (see Table 2) suggests that this intermediate can be understood

TABLE 2: Main Geometrical Data of the Structures

| structure	distance (Å)											angle (deg)	dihedral angle (deg)	
	C1–C2	C2–N3	N3–C4	C4–C5	C5–C6	C6–C1	N15–C7	C7–O8	O10–H23	C6–C7	C5–O10	C6–C7–N15	C1–C6–C7–N15	C1–C2–N3–C4
1	1.387	1.349	1.328	1.410	1.412	1.407	2.911	1.241	0.987	1.461	1.345	104.4	71.1	0.0
2	1.396	1.343	1.335	1.410	1.413	1.396	1.681	1.324	1.192	1.511	1.341	104.7	86.2	−0.5
3	1.392	1.347	1.330	1.426	1.423	1.400	1.590	1.372	1.658	1.503	1.314	107.8	93.9	−0.1
4	1.394	1.342	1.334	1.412	1.414	1.399	1.531	1.392	1.844	1.515	1.342	109.5	99.9	−0.6
5	1.395	1.340	1.334	1.404	1.410	1.400	1.463	1.429	3.166	1.526	1.359	113.0	99.9	0.6
6	1.389	1.352	1.325	1.434	1.433	1.409	1.343	1.907	2.844	1.473	1.296	120.3	20.6	0.8
7	1.367	1.377	1.304	1.467	1.459	1.432	1.326	3.454	3.618	1.404	1.258	126.5	3.4	0.7
8	1.389	1.351	1.324	1.440	1.436	1.405	1.292	3.089	3.610	1.464	1.284	121.4	92.6	0.0
9	1.373	1.368	1.312	1.451	1.447	1.424	1.314	4.226	2.907	1.413	1.271	125.4	179.6	0.0
10	1.387	1.351	1.328	1.417	1.425	1.407	1.292	4.595	3.437	1.448	1.324	119.1	178.9	0.1
11	1.392	1.344	1.333	1.403	1.413	1.403	1.281	4.396	3.574	1.465	1.357	121.1	176.8	0.1
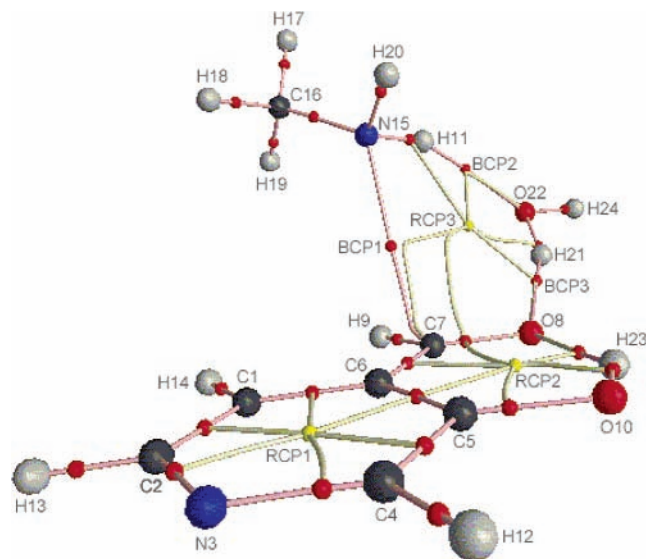
Figure 2. Molecular graph of the starting point structure **1**, showing the bond critical points, ring critical points and paths connecting them.
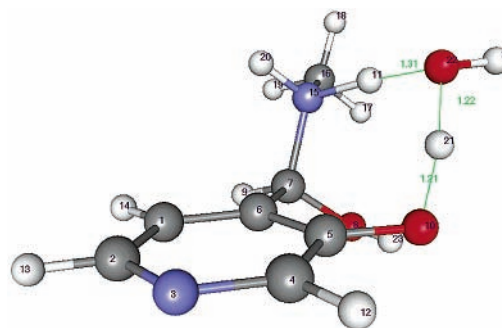

Figure 3. Perspective view of TS**4**, the concerted transition state structure previous to the formation of the main intermediate of the reaction, carbinolamine **5**.

as a zwitterionic form, where the incoming N15, because of its approximation to C7 (1.590 Å), bears a positive formal charge while O10 remains formally negatively charged because of the transference of proton H23 to O8. Also, as a result of this transference, H21 forms a hydrogen bond with O10 (1.649 Å) and changes the former orientation to O8 that had in 1 and TS2.

From this intermediate, the carbinolamine can be formed if N15 is deprotonated. The most reasonable target for the proton transfer from the amine is O10. However, the distance of any of the hydrogen atoms of the amine group to O10 (3.931 Å from H20 and 2.888 Å from H11) is far too long to allow a direct transfer. This is the point where the auxiliary water molecule plays a reactive role. The hydrogen transfer from N15 to O10 is performed through a concerted transition state represented by TS**4** (Figure 3) in which the water molecule exchanges one of its hydrogens (H21) by one of the amine (H11) and simultaneously releases the former to O10, thus regenerating the hydroxyl group bond to C5 and yielding the carbinolamine intermediate **5** once the energy gap of 4.95 kcal/mol of this transition state structure has been surmounted. The molecular graph of structure 5 (Figure 4) shows that it is highly networked by hydrogen bonds. Even a fourth RCP4 appears connected to the surrounding BCPs by ring–bond paths. The occurrence of such a highly networked topology for the electronic density function appears to be related to the stability of the structure along the reaction pathway.

B. Dehydration. Once the carbinolamine has been formed, the next step requires de dehydration of the molecule. This is
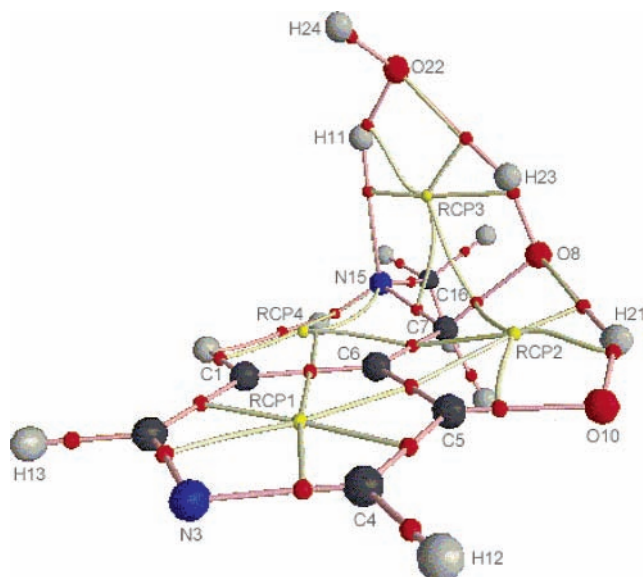
DFT Studies on Schiff Base Formation

J. Phys. Chem. A, Vol. 107, No. 44, 2003 **9413**

Figure 4. Molecular graph of structure **5**, showing the bond critical points, ring critical points and paths connecting them.
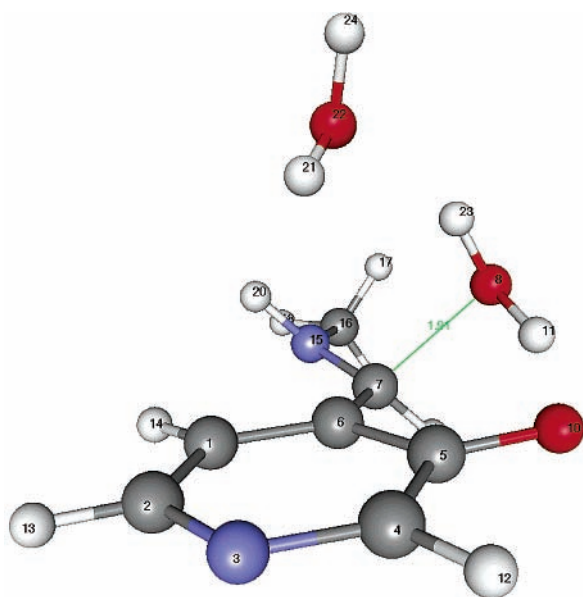

Figure 5. Perspective view of TS**6**, the limiting reaction step (dehydration).

accomplished by means of the transfer of the hydroxyl proton H21 to O8 in TS**6** (Figure 5). The water molecule assists this transfer from the top by forming a hydrogen bond directed to H23 (O22−H23, 1.918 Å). The modification of the hydrogen bond network around the atoms involved in the breakdown of C7−O8 that will result in the dehydration results in a different topology of the density charge for TS**6** if the molecular graph of this structure is compared with that of **5**. As it is displayed in the energy profile of the reaction (Figure 1), this is the highest energy barrier of the reaction path (0.031129 au, 19.5 kcal/mol), which is in accordance with the experimental observation that dehydration is the limiting step of the reaction.[9−11]

Downhill from TS**6** the dehydrated quinonoid-like intermediate **7** is formed. The ellipticity value of the BCP in C6−C7 (ϵ = 0.205) reveals an increase in π population along this bond with respect to the previous intermediate **5** (ϵ = 0.054 for the BCP of bond C6−C7). Ellipticities of BCPs regarding the bonds of the ring through the imine form (with values ranging from 0.10 to 0.30) justify the drawing of the quinonoid resonance

form of this structure in Scheme 1. The released water molecule forms a hydrogen bridge bond with the former hydroxyl oxygen O10 (H21−O10, 1.723 Å) and the already existing water molecule (O8−H11, 1.776 Å). The formation of quinonoid species as transient intermediates in the formation of Schiff bases of pyridoxal or pyridoxal derivatives with free amine containing molecules are described in absorption spectra studies.[43−45]

C. Schiff Base Formation. N15 in intermediate **7** needs to be dehydrogenated in order to form the Schiff base. What is expected is a process that would regenerate the hydroxyl group and produce the imine group C7=N15. This can be accomplished by means of the transfer of H20 to O10, although the relative orientation of H20 with respect to O10 does not allow this step to be performed directly from intermediate **7**. One of the consequences of the quinonoid-like structure of this intermediate is the lack of free rotation around the C6−C7 bond. For this reason, a rotation barrier, represented by TS**8**, must be surmounted (0.02747605 au, 17.2 kcal/mol) to yield intermediate **9**, in which H20 will point to O10. This is a low value for a rotational barrier of a C=C bond, and it can be explained for this particular step if the contribution of the zwitterionic resonant form of intermediate **7** is taken into account. This energy gap is lower than the one of the dehydration step and it is a consequence of the calculation of the molecular complex in gas phase. In water solution this transition state can be presumably avoided if the hydrogen that has to be transferred to O10 has its origin in a water molecule of the solvation sphere close to this latter atom.

Intermediate **9** as drawn is Scheme 1 is the zwitterionic form of the Schiff base. The hydrogen transfer through TS**10** regenerates the hydroxyl group bound to C5 of the pyridine ring to form the final product **11** (enolimine tautomer). However, the energy profile of the reaction reveals that the zwitterionic form **9** has a lower energy than **11** (0.00481218 au, 3.02 kcal/mol). It is known that form **9** of Schiff bases is the predominant resonance form in water and other high dielectric solvents, while solvents of low polarity favor the less polar enolimine tautomer **11**.[22] Thus, the lower energy computed for **9** can be related to the presence of the two auxiliary water molecules which results in the hydrogen bond network formed in the molecular complex. The comparison of the topology of charge density between structures **9** and **11** shows a similar distribution of RCPs for both structures and for **9** an increase in the number of paths connecting RCPs and BCPs between the Schiff base and the surrounding pair of water molecules than in **11**. This difference stands for a preferred orientation of the water molecules around the zwitterionic form of the Schiff base.

IV. Conclusions

We concluded from the previous PM3 study of the Schiff base formation of a vitamin B$_6$ analogue[33] that the carbinolamine is the main intermediate and that dehydration is the limiting step of the reaction, and pointed out the known experimental fact that the progress of the Schiff base formation depends on the polarity of the solvent, as far as internal hydrogen transfers, are involved. This DFT study has also reached similar conclusions, although the use of this level of theory has allowed the location of the concerted transition state TS**4**, which permits the consideration of 11 structures involved in the reaction path, instead of the 15 structures found in the PM3 level. The results are also in accordance with the experimental knowledge of the existence of general acid catalysis related to the phenolic O10.

As expected, the zwitterionic tautomer of the Schiff base is more stable if water is in the solvation layer. However, this

study shows that the influence of water in the formation of a Schiff base between a pyridoxal phosphate analogue and an amino acid analogue is beyond its role as a solvent. A water molecule takes part in the reaction by performing a hydrogen transfer between distant sites by means of the formation of a concerted transition state structure that allows the nucleophilic attack of the incoming amine on to the carbonyl group of the pyridoxal. Thus, water contribution to the progress of the Schiff base formation is not restricted only to solvation effects, but also acts as a reactive species. Bader's analysis of the structures found reveals complex changes on the distribution of the density charge within the molecular system formed by the substrate and the auxiliary water molecule. The evidence of the formation of ring critical points associated to networks of hydrogen bonds at distances larger than the standard (as shown by the existence of BCPs) suggest that the role of such interactions is important, and provides a point of view for understanding the influence of the solvent on the progress of the reaction.

References and Notes

(1) Adams, E. *Adv. Enzymol.* **1976**, *44*, 69.

(2) Akhtar, M.; Emery, V. C.; Robinson, J. A. In *New Comprehensive Biochemistry*; Neuberger, A., Ed.; Elsevier Science: Amsterdam, 1984; Vol. 6.

(3) Evangelopoulos, A. E. In *Chemical and Biological Aspects of Vitamin B6 Catalysis*; Liss, R. A., Ed.; New York, 1984.

(4) Christen, P.; Metzler, D. E. In *Transaminases*; John Wiley: New York, 1985.

(5) Snell, E. E. In *Vitamin B6 Pyridoxal Phosphate, Chemical, Biochemical and Medical Aspects*; Dolphin, D., Poulson, R.; Avramovic, O., Eds.; Wiley-Interscience: New York, 1986; Part A.

(6) Metzler, D. E.; Ikawa, M.; Snell, E. E. *J. Am. Chem. Soc.* **1954**, *76*, 648.

(7) Braunstein, A. E.; Shenyakin, M. M. *Biokhimiia* **1953**, *18*, 393.

(8) Jencks, W. In *Catalysis in Chemistry and Enzymology*; McGraw-Hill: New York, 1969.

(9) Sayer, J. M.; Pinsky, B.; Schonbrunn, A.; Washtien, W. *J. Am. Chem. Soc.* **1974**, *96*, 7998.

(10) Sayer, J. M.; Jenks, W. P. *J. Am. Chem. Soc.* **1977**, *99*, 464.

(11) Sayer, J. M.; Conlon, P. *J. Am. Chem. Soc.* **1980**, *102*, 3592.

(12) Jenkins, W. T.; D'Ari, L. *J. Biol. Chem.* **1996**, *241*, 5667.

(13) Golichowski, A.; Jenkins, W. T. *Arch. Biochem. Biophys.* **1977**, *178*, 459.

(14) Nichol, L. W.; Ogston, A. G.; Winzor, D. J.; Sawyer, W. H. *Biochem. J.* **1974**, *143*, 435.

(15) Dunn, B. M.; Chaiken, I. M. *Proc. Natl. Acad. Sci. (USA)* **1974**, *71*, 2382.

(16) Morozov, Y. V. In *Vitamin B6 Pyridoxal Phosphate, Chemical, Biochemical and Medical Aspects*; Dolphin, D., Poulson, R., Avramovic, O., Eds.; Wiley-Interscience: New York, 1986; Part A,

(17) Mandeles, S.; Koppelman, R.; Hanke, M. E. *J. Biol. Chem.* **1954**, *209*, 327.

(18) Cortijo, M.; Llor, J.; Sanchez Ruiz, J. M. *J. Biol. Chem.* **1988**, *263*, 17960.

(19) Martell, A. E. *Acc. Chem. Res.* **1989**, *22*, 115.

(20) Martell, A. E. In *Chemical and Biological Aspects of vitamin B-6 Catalysis*; Evangelopoulos, A., Ed.; A. R. L.: New York, 1984; Part A.

(21) Martell, A. E. *Adv. Enzymol.* **1982**, *53*, 163.

(22) Metzler, C. M.; Cahill, A.; Metzler, D. E. *J. Am. Chem. Soc.* **1980**, *102*, 6075.

(23) Vàzquez, M. A.; Muñoz, F.; Donoso, J.; García-Blanco, F. *Biochem J.* **1991**, *279*, 759.

(24) Vàzquez, M. A.; Muñoz, F.; Donoso, J.; García-Blanco, F. *Helv. Chim. Acta* **1992**, *75*, 1029.

(25) Vázquez, M. A.; Donoso, J.; Muñoz, F.; García-Blanco, F.; García del Vado, M. A.; Echevarria, G. *J. Chem. Soc., Perkin Trans.* **1991**, *2*, 1143.

(26) Vázquez, M. A.; Muñoz, F.; Donoso, J.; García-Blanco, F. *Biochem. (Life Sci. Adv.)* **1992**, *11*, 241.

(27) Vázquez, M. A.; Muñoz, F.; Donoso, J.; García-Blanco, F. *Amino Acids* **1992**, *3*, 81.

(28) Morozov, Y. V.; Almazov, V. P.; Savin, F. A.; Bazhulina, N. P. *Bioorganitek. Khim.* **1992**, *8*, 1119.

(29) Nero, T. L.; Iskander, M. N.; Wong, M. G. *J. Chem. Soc. Perkin. Trans 2*, 1993, 431.

(30) Alagona, G.; Ghio, C.; Agresti, A. *Comput. Chem. (Oxford)* **2000**, *24*, 311.

(31) Bach, R. D.; Canepa, C.; Glukhovtsev, M. N. *J. Chem. Soc.* **1999**, *121*, 6542.

(32) Toney, M. D. *Biochemistry* **2001**, *40*, 1378.

(33) Salvà, A.; Donoso, J.; Frau, J.; Muñoz, F. *J. Mol. Struct.: THEOCHEM* **2002**, *577*, 229.

(34) Weiner, S. J.; Singh, U. C.; Kollman, P. A. *J. Am. Chem. Soc.* **1985**, *97*, 2219.

(35) Frau, J.; Donoso, J.; Muñoz, F.; García-Blanco, F. *J. Comput. Chem.* **1992**, *13*, 681.

(36) Frau, J.; Donoso, J.; Vilanova, B.; Muñoz, F.; García-Blanco, F. *Theor. Chim. Acta* **1993**, *86*, 229.

(37) Frisch, M. J.; Trucks, G. W.; Schlegel, H. B.; Gill, P. M. W.; Johnson, B. G.; Robb, M. A.; Cheeseman, J. R.; Keith, T.; Petersson, G. A.; Montgomery, J. A.; Raghavachari, K.; Al-Laham, M. A.; Zakrzewski, V. G.; Ortiz, J. V.; Foresman, J. B.; Cioslowski, J.; Stefanov, B. B.; Nanayakkara, A.; Challacombe, M.; Peng, C. Y.; Ayala, P. Y.; Chen, W.; Wong, M. W.; Andres, J. L.; Replogle, E. S.; Gomperts, R.; Martin, R. L.; Fox, D. J.; Binkley, S. J.; Defrees, D. J.; Baker, J.; Stewart, J. P.; Head-Gordon, M.; Gonzalez, C.; Pople, J. A. *Gaussian 94*, revision D.4; Gaussian, Inc.: Pittsburgh, PA, 1995.

(38) Becke, A. D. *J. Chem. Phys.* **1993**, *98*, 5468.

(39) Lozynshi, M.; Rusinska-Roszak, D.; Mack, H. G. *J. Chem. Phys.* **1997**, *101*, 1542.

(40) Kim, K.; Jordan, K. D. *J. Chem. Phys.* **1994**, *98*, 10089.

(41) Bader, R. F. W. In *Atoms in Molecules: A Quantum Theory*; Clarendon Press: Oxford, England, 1990.

(42) Biegler-König, F.; Schönbohm, J.; Bayles, D. *J. Comput. Chem.* **2001**, *22*, 545.

(43) Schirch, L.; Slotter, R. *Biochemistry* **1966**, *5*, 3175

(44) Abbot, E. A.; Bobrik, A. *Biochemistry* **1973**, *12*, 846.

(45) Maley, J. R.; Bruice, T. C. *J. Am. Chem. Soc.* **1983**, *90*, 2843.